

Cite this: *Mater. Adv.*, 2023,  
4, 4921

# Dicyano-functionalized indium framework as a heterogeneous catalyst for CO<sub>2</sub> fixation in the absence of solvent and co-catalyst†

Naghmeh Bayati  and Saeed Dehghanpour \*

Catalytic carbon dioxide (CO<sub>2</sub>) transformation into valuable products is of great interest, especially the development of innovative methods for CO<sub>2</sub> fixation reactions. In this paper, we report the porous cyanide-functionalized MIL-68(In) metal–organic framework as a novel Lewis acid–base bifunctional catalyst. The MIL-68(In) framework was modified with different cyanide functional groups, such as 1,3-phenylene diacetonitrile and malononitrile, for the catalytic CO<sub>2</sub> fixation reaction into cyclic carbonates. The properties of the synthesized catalysts were fully characterized using different techniques, including PXRD, FTIR, N<sub>2</sub> adsorption, BET, SEM, XPS, TGA, NH<sub>3</sub>-TPD, and CO<sub>2</sub>-TPD. Under the optimized conditions (30 mg catalyst, 1 MPa CO<sub>2</sub> pressure, 20 mmol epichlorohydrin, 100 °C, 10 h), MIL-68(In) functionalized with 1,3-phenylene diacetonitrile was found to afford a remarkable heterogeneous catalyst with selectivity (100%) and high conversion (99%) for the coupling reaction between CO<sub>2</sub> and the epoxide without any co-catalyst or solvent. Moreover, the functionalized MIL-68(In) MOF also revealed applicability to other large epoxides. The enhanced activity of functionalized MIL-68(In) results from the collaboration between the unsaturated Lewis acidic indium centers and cyanide functional groups as nucleophilic sites. Furthermore, the reusability tests demonstrated that the modified MIL-68(In) was easily recycled by filtration and reusable for at least five runs with no loss in catalytic ability.

Received 8th August 2023,  
Accepted 31st August 2023

DOI: 10.1039/d3ma00513e

rsc.li/materials-advances

## 1. Introduction

Nowadays, the increasing carbon dioxide (CO<sub>2</sub>) concentration in the atmosphere resulting from fossil fuels has received much attention from the viewpoint of greenhouse gas emissions and atmospheric temperature in the 21st century.<sup>1</sup> Therefore, it is necessary to develop effective technologies to transform CO<sub>2</sub> from a renewable raw material (a non-toxic, and non-flammable abundant gas) into useful chemicals, aiding in greenhouse gas reduction.<sup>2–4</sup> In particular, the coupling reaction of carbon dioxide with an epoxide is highlighted as a highly appreciated economic reaction, and the cyclic carbonate products are widely used as pharmaceutical intermediates, precursors for polycarbonates, and other polymeric materials.<sup>5–7</sup> Because of the high thermodynamic stability of the cycloaddition reaction, the promotion of CO<sub>2</sub>–epoxide couplings requires effective catalysts and high temperature or pressure conditions.<sup>8–10</sup> The natural solubility of homogeneous catalysts hinders the particular functions of many advanced catalysts for CO<sub>2</sub> transformation.<sup>6</sup> So, the

utilization of heterogeneous catalysts is imperative due to their simple separation method, sample treatment, and reusability.<sup>11</sup>

Hence, catalytic systems incorporating acidic sites for epoxide electrophilic activity and basic sites as nucleophilic species are of interest for the CO<sub>2</sub>-to-epoxide coupling reaction.<sup>12</sup>

In general, metal–organic frameworks (MOFs) have attracted lots of attention in the field of catalysis due to their large specific surface areas, high CO<sub>2</sub> adsorption capacities, tailorable porosity, diverse compositions, high catalytic performance, and controllable open channels and pores.<sup>13–16</sup> Many MOFs have been developed for CO<sub>2</sub>-to-epoxide couplings because MOFs can provide Lewis acid–base sites, which are noted for the facilitation of CO<sub>2</sub> cycloaddition reactions.<sup>17–21</sup> Moreover, a co-catalyst or additives containing halide anions are frequently used in CO<sub>2</sub> chemical conversion.<sup>22</sup> In addition, the development of metal–organic frameworks that can be used as catalysts in CO<sub>2</sub> cycloaddition reactions with no need for a co-catalyst or additives has gained tremendous attention.

It has been shown that indium, a metal with accessible high-level p-orbitals, is capable of receiving electrons in different Lewis acid reactions.<sup>23</sup> Owing to this unique electronic configuration, it is reported that indium MOFs have been synthesized with a high surface area and found to possess a porous structure of high chemical and thermal stability. The use of some of them,

Department of Inorganic Chemistry, Faculty of Chemistry, Alzahra University, Tehran, Iran. E-mail: Dehghanpours@alzahra.ac.ir

† Electronic supplementary information (ESI) available. See DOI: <https://doi.org/10.1039/d3ma00513e>



such as CPM-23-In, CPM-200-In and In-MOF, as catalysts for selective and high CO<sub>2</sub> uptake in the chemical fixation of CO<sub>2</sub> with epoxides has also been demonstrated previously.<sup>23–26</sup>

The purpose of the work presented herein was to eliminate the addition of a co-catalyst, and instead incorporate nucleophilic functional groups into the structure to play the co-catalyst role for the CO<sub>2</sub> fixation reaction. The application of different functional groups in stable MOF structures for the special properties that arise from this modification has previously been investigated.<sup>27–32</sup>

With these considerations in mind and the importance of modified MOFs, we used cyanide groups as a co-catalyst to design a novel cyanide-functionalized MIL-68(In) structure that is assembled from InO<sub>4</sub>(OH)<sub>2</sub> octahedral units linked to each other with terephthalate ligands. Volklinger and coworkers found that MIL-68(In) displays large surface area and high thermal stability.<sup>33</sup> MIL-68(In) showed two kinds of triangular and hexagonal channels (with pore diameters of 6.0 and 16.0 Å, respectively). In addition, the structure of MIL-68(In) leads to the arrangement of the functional groups within the pores in the modified MIL-68(In).<sup>30,34–36</sup> Thus, the latter strategy was the synthesis of a CN-functionalized porous MIL-68(In) framework. We designed and synthesized two cyanide-functionalized MIL-68(In) MOFs with acidic and basic sites in the framework, which were then used in the catalytic CO<sub>2</sub> transformation reaction (Scheme 1). The two new cyanide-modified MIL-68(In) MOFs were prepared by hydrothermal methods and identified by various techniques, such as PXRD, FTIR, SEM, TGA, BET, XPS, and N<sub>2</sub> and CO<sub>2</sub> adsorption measurements. The catalytic activity of the cyanide-modified frameworks were tested under low pressure and temperature (mild conditions) in the absence of a co-catalyst or solvent. The effects of various reaction parameters, activities over different substrates, and catalyst recyclability were

investigated and are reported below. The results show that modification with cyanide groups causes a great improvement in the conversion of epoxides and CO<sub>2</sub> to cyclic carbonates.

## 2. Experimental

### 2.1. Materials

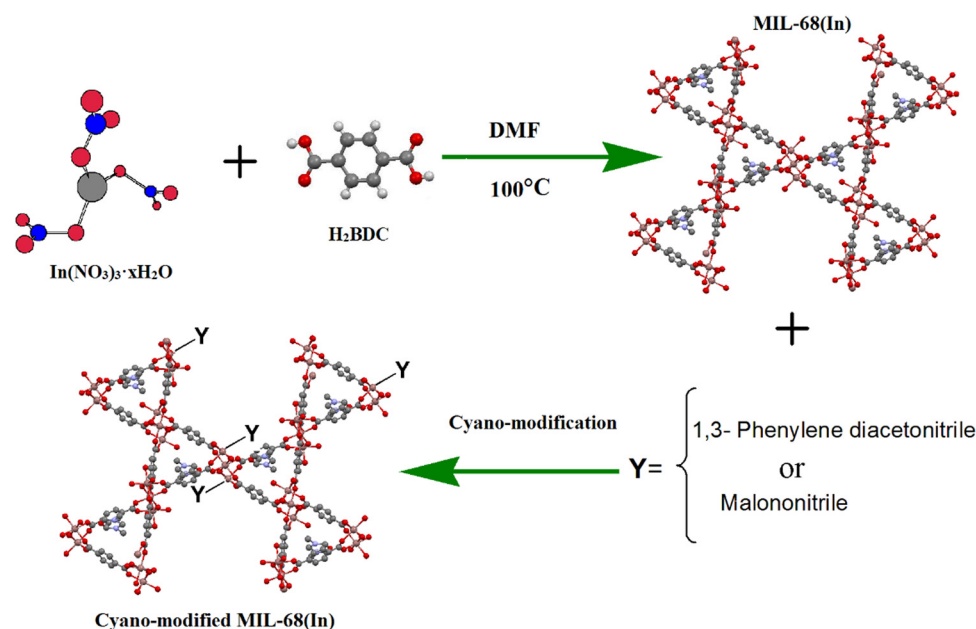
All solvents and chemicals employed in this work are described in the ESI.†

### 2.2. Preparation of catalysts

**2.2.1. Synthesis of MIL-68(In).** The synthesis of MIL-68(In) was done based on the previously reported method.<sup>33</sup> In a typical process, In(NO<sub>3</sub>)<sub>3</sub>·xH<sub>2</sub>O (408.2 mg, 1.05 mmol) and 1,4-benzenedicarboxylic acid (H<sub>2</sub>BDC) (200 mg, 1.20 mmol) were added to *N,N*-dimethylformamide (DMF) (200 mg, 1.20 mmol). The mixture was sealed in a 15 ml Teflon-lined stainless steel autoclave and heated for 48 h at 100 °C in an oven. The obtained white precipitate consisted of needle-like crystallites that were washed with DMF and immersed in absolute ethanol for several days and the solvent was refreshed once a day to remove the guest molecules in the pores. Finally, the product was filtered and dried in a vacuum oven at 50 °C overnight.

**2.2.2. Synthesis of MIL-68(In)-PhDA.** MIL-68(In)-PhDA was prepared by the post-synthetic process. Typically, 0.52 g of activated MIL-68(In) was stirred into 25 ml of toluene and suspended in 1,3-phenylene diacetonitrile (PhDA) (0.5 g, 3.20 mmol) and dichloromethane (CH<sub>2</sub>Cl<sub>2</sub>) (25 ml) and then refluxed for 20 h. Finally, the filtered precipitate was collected and dried in a vacuum oven at 90 °C for 4 h.

**2.2.3. Synthesis of MIL-68(In)-malo.** This catalyst was synthesized by a similar protocol, except for the use of 0.15 g



Scheme 1 Schematic representation of 1,3-phenylene diacetonitrile MIL-68(In)-PhDA and MIL-68(In)-malo synthesis.



(2.27 mmol) malononitrile (malo) instead of 1,3-phenylene diacetonitrile and all other conditions were kept unaltered.

### 2.3. Catalytic reaction: CO<sub>2</sub> fixation

In order to eliminate the solvent molecules, the MOF catalysts were activated at 120 °C for 12 h. In a typical run, an epoxide (20 mmol) and 30 mg of sample were put into a 25 ml autoclave. Then, the reactor was pressurized with CO<sub>2</sub> up to 1 MPa when the system attained the point reaction temperature (100 °C for 10 h). After the end of the reaction, the reactor was slowly cooled down to room temperature and degassed. The products were extracted and analyzed by gas chromatography (GC).

## 3. Results and discussion

### 3.1. Characterization

The powder X-ray diffraction (PXRD) patterns of the synthesized MIL-68(In), MIL-68(In)-PhDA, and MIL-68(In)-malo frameworks are presented in Fig. S1 (ESI<sup>†</sup>). The diffraction peaks of the samples are similar and no differences can be observed owing to

the same crystalline structures. This further verifies that modification of the framework with cyanide functional groups does not disrupt the structural integrity of MIL-68(In) and the basic diffraction peaks remain intact upon CN-functionalization.

The FTIR spectra of the synthesized MIL-68(In), MIL-68(In)-PhDA, and MIL-68(In)-malo frameworks are shown in Fig. S2 (ESI<sup>†</sup>). The typical absorption bands in the range of 1400–1700 cm<sup>-1</sup> are related to the symmetric and asymmetric stretching vibrational modes of the carboxylate groups.<sup>37</sup> The appearance of a cyanide (-CN) peak, related to the modified framework, becomes clear at around 2253 cm<sup>-1</sup> and confirms the introduction of the cyanide groups into the framework.<sup>38</sup> The observed broad band in the region of 2900–3600 cm<sup>-1</sup> can be assigned to the stretching vibration of H<sub>2</sub>O molecules coordinated with the metal center.

To characterize the textural morphology of the as-prepared frameworks, scanning electron microscopy (SEM) analysis was performed. As shown in Fig. S3 (ESI<sup>†</sup>), all of the samples reveal needlelike structures and the morphology is preserved even after modification with cyanide groups.

The thermogravimetric analysis (TGA) was conducted under a nitrogen atmosphere and the results are shown in Fig. S4

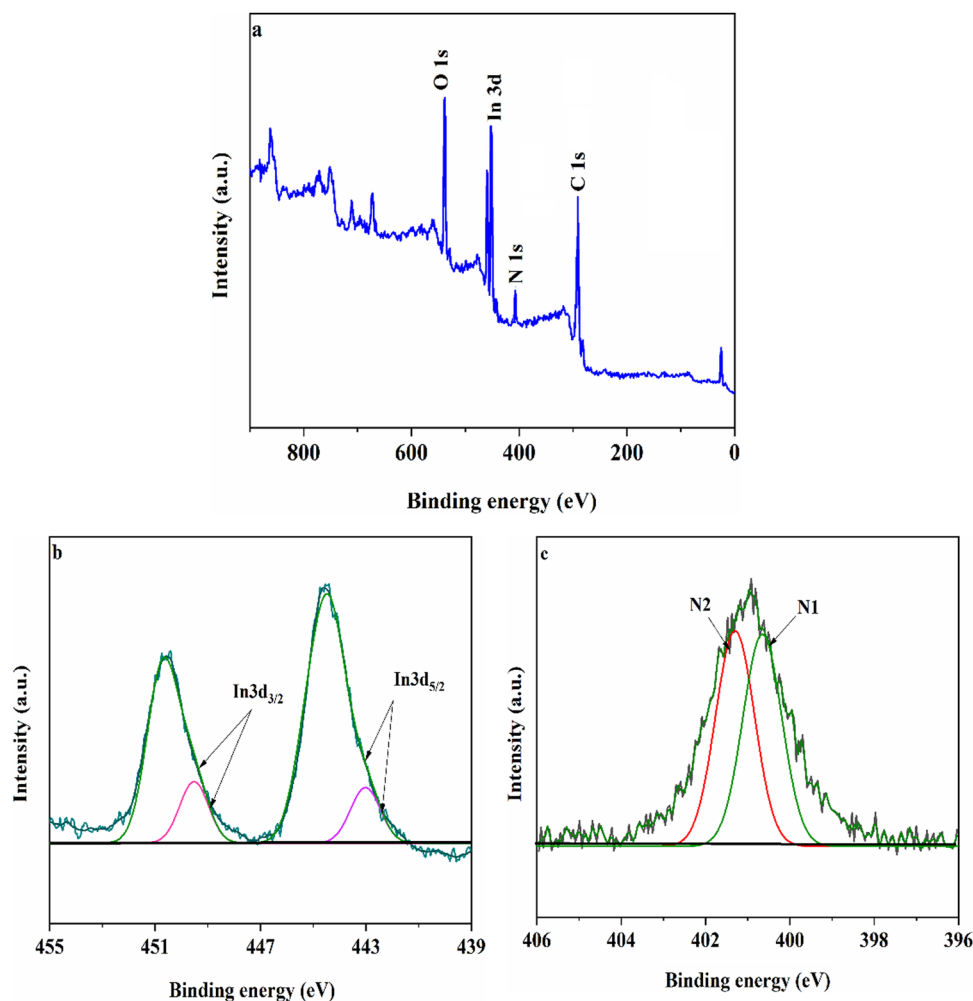


Fig. 1 Typical XPS survey spectra of MIL-68(In)-PhDA (a), In 3d spectra (b) and N 1s spectra (c) of MIL-68(In)-PhDA.



(ESI<sup>†</sup>). The TGA curve of MIL-68(In) presents two weight losses. The first weight loss below 110 °C is due to the removal of trapped solvent molecules. The framework is stable at nearly 450 °C, then decomposes. TGA analysis was also performed on the modified frameworks. All of the modified structures are stable up to 450 °C. The first weight loss has disappeared due to the removal of trapped solvent in the modified frameworks. This obviously shows the effective elimination of the guest molecules and the successful functionalization of the frameworks.<sup>30</sup>

To verify the interaction environment of the elements and cyanide functional groups in modified Mil-68(In), X-ray photoelectron spectroscopy (XPS) analysis was performed and the results are presented in Fig. 1. As seen in Fig. 1(a), the survey spectrum of MIL-68(In)-PhDA clearly shows the main peaks of O, In, N, and C elements. In Fig. 1(b), the In 3d spectrum shows two types of peaks, In 3d<sub>5/2</sub> (444.6 eV) and In 3d<sub>3/2</sub> (450.4 eV).<sup>39</sup> The two peaks for In 3d<sub>5/2</sub> and In 3d<sub>3/2</sub> could be resolved into satellite peaks at binding energies of 442.8 and 449.4 eV, respectively, which can be assigned to the 1,3-phenylene diacetonitrile functional groups in the modified MIL-68(In).<sup>40</sup> As can be seen from Fig. 1(c), two types of N (denoted as N1 and N2) appeared at 399.8 (CN-C-) and 401.1 eV (C-N-In).<sup>41</sup>

N<sub>2</sub> adsorption-desorption isotherms of the functionalized compounds are depicted in Fig. 2, and all of the compounds reveal a type I isotherm characteristic of the microporous nature. A Brunauer-Emmett-Teller (BET) specific surface area of 1058 m<sup>2</sup> g<sup>-1</sup> and pore volume of 0.59 cm<sup>3</sup> g<sup>-1</sup> were found for MIL-68(In), and the corresponding values for the other modified samples are shown in Table 1. The decrease in the BET surface area and pore volume supports the conclusion that the frameworks have been functionalized.

To evaluate the CO<sub>2</sub> adsorption properties of the cyanide-modified structures, CO<sub>2</sub> measurements were performed (Fig. 3).

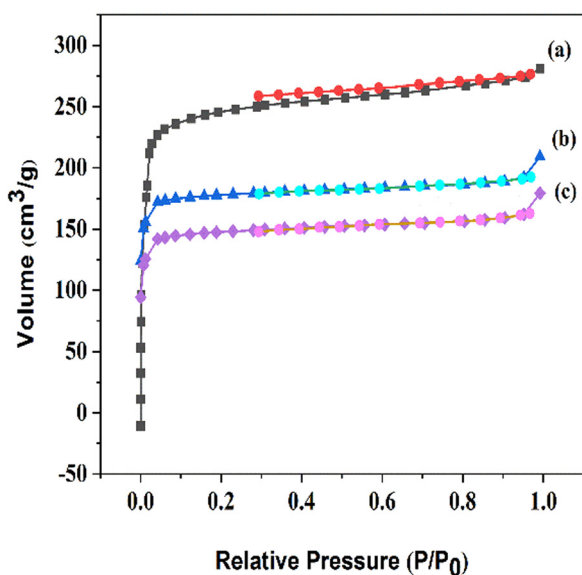


Fig. 2 N<sub>2</sub> adsorption-desorption isotherms of (a) MIL-68(In), (b) MIL-68(In)-malo, and (c) MIL-68(In)-PhDA.

Table 1 Textural properties of MIL-68(In), MIL-68(In)-malo, and MIL-68(In)-PhDA

Sample	S <sub>BET</sub> (m <sup>2</sup> g <sup>-1</sup> )	Pore volume (cm <sup>3</sup> g <sup>-1</sup> )
MIL-68(In)	1058	0.59
MIL-68(In)-malo	814	0.37
MIL-68(In)-PhDA	623	0.29

The CO<sub>2</sub> sorption capacity of MIL-68(In) is 35 cm<sup>3</sup> g<sup>-1</sup> and this increased up to 48 cm<sup>3</sup> g<sup>-1</sup> for MIL-68(In)-malo and 51 cm<sup>3</sup> g<sup>-1</sup> for MIL-68(In)-PhDA. The incorporation of the cyanide functional groups into the framework are responsible for the increase in the CO<sub>2</sub> uptake capacity. Therefore, the high affinity of the functionalized structure for CO<sub>2</sub> adsorption affirms the modification of the framework.

To investigate the acid-base characteristics of the MOF materials, we used temperature programmed desorption (TPD) analysis. The NH<sub>3</sub> desorption peak profile (Fig. 4a) at about 300 °C might be related to uncoordinated Lewis acid sites. Furthermore, in the case of the CO<sub>2</sub>-TPD results (Fig. 4b) for MIL-68(In)-PhDA, the peaks at about 320 °C are attributed to the strong basic sites of the cyanide functional groups in the structure.

The C, H, and N contents of various samples were measured to determine the amount of each element and the catalyst loadings. The values of cyanide loaded in the modified samples were 22.59% (MIL-68(In)-PhDA) and 8.89% (MIL-68(In)-malo) (Table S1, ESI<sup>†</sup>), and this confirmed the modification of the structure with cyanide groups.

### 3.2. Catalytic activity in the CO<sub>2</sub> fixation reaction

In order to investigate the catalytic ability of MIL-68(In), MIL-68(In)-PhDA, and MI-68(In)-malo in the CO<sub>2</sub> fixation reaction, epichlorohydrin (ECH) epoxide was applied as the model substrate.

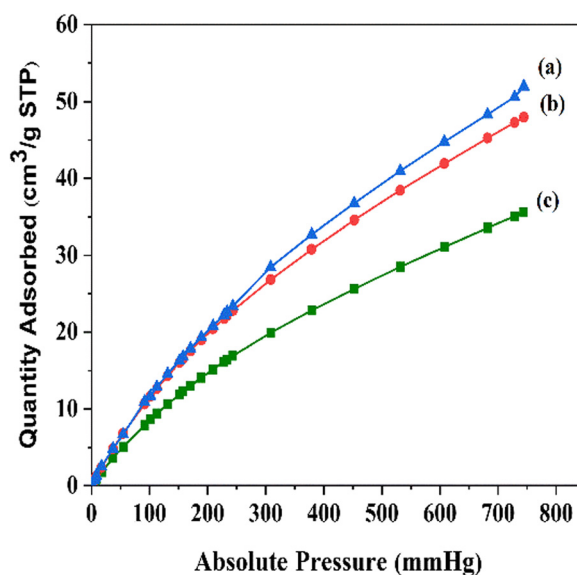


Fig. 3 CO<sub>2</sub> sorption isotherms of (a) MIL-68(In)-PhDA, (b) MIL-68(In)-malo, and (c) MIL-68(In) at 298 K.



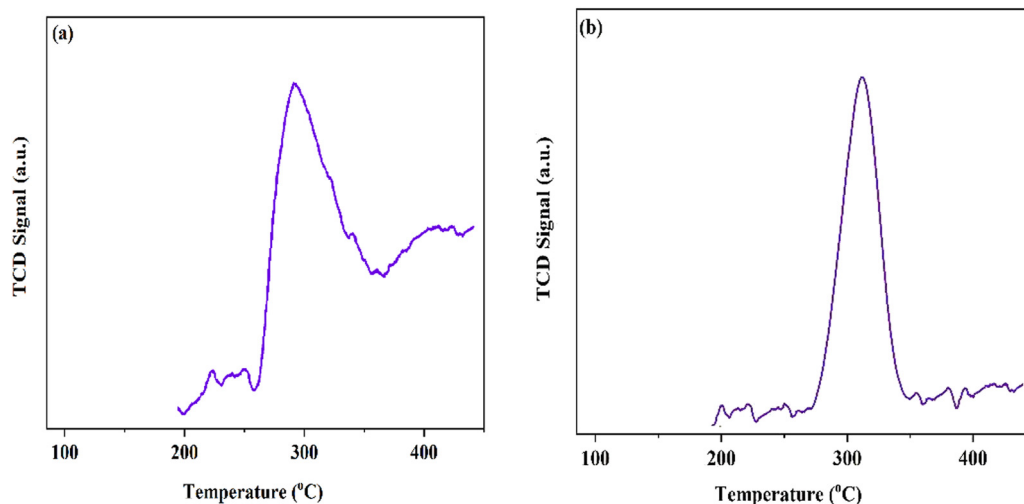


Fig. 4 (a)  $\text{NH}_3$  and (b)  $\text{CO}_2$  temperature programmed desorption plots of MIL-68(In)-PhDA.

Additionally, we clarified the role of the cyanide functional group in the modified materials as co-catalyst. The data are shown in Table 2 and evaluated against a blank experiment that was performed in the absence of a catalyst. According to the results, the reaction did not give any ECH conversion without the catalyst (Table 2, entry 1). Moreover, using the pristine MOF (MIL-68(In)) or 1,3-phenylene diacetonitrile (PhDA) alone do not lead to significant enhancement of the cycloaddition reaction (Table 2, entries 2 and 3). The conversion of catalyst was clearly enhanced by cyanide functionalization (Table 2, entry 5). Also, the physical combination of MIL-68(In) with 1,3-phenylene diacetonitrile slightly increases the conversion achieved (27%). It can be seen that modification of MIL-68(In) with cyanide functional groups improves the performance of the catalyst without adding solvent or a co-catalyst.

The values of  $\text{CO}_2$  pressure, reaction temperature, catalyst amount, and reaction time were optimized for the catalytic performance. The results are shown in Fig. S5–S8 (ESI<sup>†</sup>), respectively. It can be seen that the conversion of ECH to epichlorohydrin carbonate (ECHC) was 99% over MIL-68(In)-PhDA catalyst under optimal conditions.

### 3.3. Catalytic performance of the prepared compounds

The catalytic ability of modified catalysts (MIL-68(In)-PhDA as 1 and MIL-68(In)-malo as 2) was tested for the chemical fixation reaction. Based on the successful catalytic performance of MIL-68(In)-PhDA in the conversion of ECH, cycloaddition reactions

Table 2 The catalytic activity of different catalysts

Entry	Catalyst	Conv. (%)
1	Blank	—
2	MIL-68(In)	15
3	1,3-Phenylene diacetonitrile	7
4	MIL-68(In)/PhDA	27
5	MIL-68(In)-PhDA	99

Reaction conditions: catalyst (30 mg), ECH (20 mmol),  $\text{CO}_2$  (1 MPa), 100 °C, 10 h.

were studied under optimized conditions using different aliphatic and aromatic epoxides, and the data are shown in Table 3. All modified catalysts (1 and 2) can efficiently convert propylene oxide (PO) to its carbonate and epoxy butane (EB) to butylene carbonate with 100% selectivity (Table 3, entries 2 and 3) due to the small size of the epoxide that can penetrate the holes and access acidic and basic sites in the functionalized catalysts. In the case of bulky epoxides, though the previously reported low conversion<sup>42</sup> is due to the high steric hindrance of the epoxide, significant conversions with high selectivity into the related carbonates are obtained for styrene oxide (SO) and cyclohexene oxide (CHO) (Table 3, entries 5 and 7). In addition, even with an increase in the molecular size of the epoxides, such as allyl glycidyl ether (AGE) and phenyl glycidyl ether (PGE), notable conversion was afforded (Table 3, entries 4 and 6).

### 3.4. Possible reaction mechanism

On the basis of the experimental results and prior studies, the synergistic role of Lewis acid–base sites is necessary for the cycloaddition of  $\text{CO}_2$  and epoxides.<sup>43,44</sup> So, a possible mechanism is suggested for the  $\text{CO}_2$  cycloaddition reaction to cyclic carbonates in Scheme 2. Accordingly, the indium atom as a Lewis acidic site initiates an electrophilic interaction with the oxygen atom of the epoxide, which is noted to activate the epoxy ring. At the same time, nucleophilic attack of the basic sites affords a sort of polar nature to the  $\text{CO}_2$  molecules (Scheme 2, route A). Now that the  $\text{CO}_2$  molecules and epoxide are activated, the ring opening of the epoxide starts with nucleophilic attack of the oxygen anion on the slightly sterically hindered epoxide side (Scheme 2, route B). Thereafter, alkyl carbonate anions are formed by the insertion of  $\text{CO}_2$  molecules (Scheme 2, route C). Finally, ring closure leads to the formation of the corresponding cyclic carbonates (Scheme 2, route D).

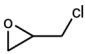
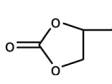
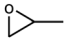
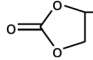
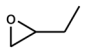
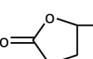
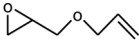
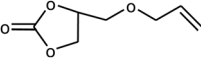
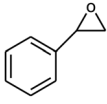
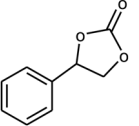
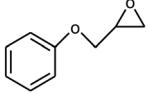
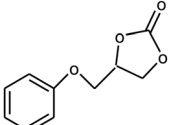
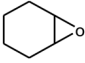
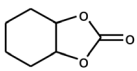
### 3.5. Comparison with other modified frameworks

The vital role of the cyanide functional group in the progress of the reaction has been clearly demonstrated. In comparison

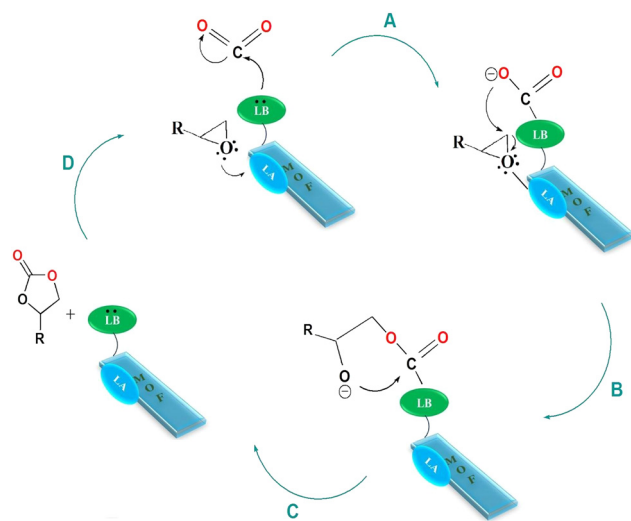




Table 3 Synthesis of cyclic carbonates from various epoxides

Entry	Epoxide	Product	Catalyst	Conv. <sup>a</sup> (%)	TON <sup>b</sup>	TOF <sup>c</sup> (h <sup>-1</sup> )
1			1	99	495	49.5
			2	97	485	48.5
2			1	94	470	47
			2	83	415	41.5
3			1	88	440	44
			2	74	370	37
4			1	71	355	35.5
			2	63	315	31.5
5			1	74	370	37
			2	70	350	35
6			1	72	360	36
			2	68	340	34
7			1	92	460	46
			2	85	425	42.5

Catalyst 1: MIL-68(In)-PhDA and catalyst 2: MIL-68(In)-malo.<sup>a</sup> Reaction conditions: catalyst (30 mg, 0.04 mmol cyanide groups), epoxides (20 mmol), CO<sub>2</sub> (1 MPa), 100 °C, 10 h. <sup>b</sup> TON (turnover number) is the mmol of product/mmol active cyanide site. <sup>c</sup> TOF (turnover frequency) is the turnover number/reaction time.



Scheme 2 Proposed mechanism for cycloaddition of CO<sub>2</sub> by modified MIL-68(In) catalyst. MOF: metal-organic framework, LA: Lewis acid, LB: Lewis base.

with catalyst 2, catalyst 1 showed the higher performance because the cyanide groups in catalyst 1 have less flexibility and are less able to rotate than in catalyst 2, so the decrease in the distance between the cyanide functional groups and the  $\beta$ -carbon of the epoxide facilitates the nucleophilic attack. Additionally, the high amount of CO<sub>2</sub> gas adsorption into the cyanide groups of

catalyst 1 (Fig. 3) followed by the positive effect on the nucleophilic attack leads to higher activity of the catalyst.

To specify the catalytic performance of the functionalized catalysts with other reported MOF catalysts, we compared the results of this work with other previously reported MOF heterogeneous catalysts for the CO<sub>2</sub>-epoxide coupling reaction. Details of the results are exhibited in Table 4. Some reports were carried out with higher CO<sub>2</sub> pressure, longer reaction times, and lower TOF than our modified catalytic systems. Therefore, MIL-68(In)-PhDA can be considered as a comparable or superior catalyst to prior reported catalysts for the chemical transformation of CO<sub>2</sub>.

### 3.6. Reusability of the catalysts

The sufficiency and recyclability of the functionalized samples for the cycloaddition reaction were examined under optimal reaction conditions (Fig. S9, ESI<sup>†</sup>). MIL-68(In)-PhDA was separated from the reaction mixture by washing with dichloromethane (CH<sub>2</sub>Cl<sub>2</sub>) and vacuum drying. As shown in Fig. S9 (ESI<sup>†</sup>), based on five catalytic cycles, the catalyst is stable with no decrease in its initial activity. The XRD pattern of the recycled MOF shows the preservation of the main diffraction peaks compared to the fresh catalysts after five cycles, which indicates that the catalyst structure was not lost during the cycloaddition reaction of epoxides (Fig. S10, ESI<sup>†</sup>). The FTIR analysis results for the recovered catalysts are the same as those of the pristine catalyst, which also confirms the structural crystallinity (Fig. S11, ESI<sup>†</sup>). Furthermore, it was observed from





- 28 M. Saghian, S. Dehghanpour and M. Sharbatdaran, *J. CO<sub>2</sub> Util.*, 2020, **41**, 101253.
- 29 Q. T. Nguyen, X. H. Do, K. Y. Cho, Y. R. Lee and K. Y. Baek, *J. CO<sub>2</sub> Util.*, 2022, **61**, 102061.
- 30 L. Wu, M. Xue, S. L. Qiu, G. Chaplais, A. Simon-Masseron and J. Patarin, *Microporous Mesoporous Mater.*, 2012, **157**, 75–81.
- 31 J. Zhang, H. Zhang, Q. Liu, D. Song, R. Li, P. Liu and J. Wang, *Chem. Eng. J.*, 2019, **368**, 951–958.
- 32 N. Bayati and S. Dehghanpour, *J. Environ. Sci.*, 2023, **132**, 12–21.
- 33 C. Volklinger, M. Meddouri, T. Loiseau, N. Guillou, M. Haouas, F. Taulelle, N. Audebrand, M. Latroche and D. V. Saint Quentin, *Inorg. Chem.*, 2008, **47**, 11892–11901.
- 34 J. Zhu, H. Zhang, Q. Liu, C. Wang, Z. Sun, R. Li, P. Liu, M. Zhang and J. Wang, *J. Taiwan Inst. Chem. Eng.*, 2019, **99**, 45–52.
- 35 T. Lescouet and D. Farrusseng, *ChemCatChem*, 2012, **4**(11), 1725–1728.
- 36 L. N. Jin, X. Y. Qian, J. G. Wang, H. Aslan and M. Dong, *J. Colloid Interface Sci.*, 2015, **453**, 270–275.
- 37 R. Liang, R. Huang, X. Wang, S. Ying, G. Yan and L. Wu, *Appl. Surf. Sci.*, 2019, **464**, 396–403.
- 38 M. Saghian, S. Dehghanpour and M. Sharbatdaran, *Appl. Catal., A*, 2021, **612**, 117982.
- 39 W. Cao, Y. Yuan, C. Yang, S. Wu and J. Cheng, *Chem. Eng. J.*, 2020, **391**, 123608.
- 40 P. Deminskyi, P. Rouf, I. G. Ivanov, H. Pedersen, P. Deminskyi, P. Rouf, I. G. Ivanov and H. Pedersen, *J. Vac. Sci. Technol., A*, 2019, **37**, 020926.
- 41 J. Zhang, H. Zhang, Q. Liu, D. Song, R. Li, P. Liu and J. Wang, *Chem. Eng. J.*, 2019, **368**, 951–958.
- 42 J. F. Kurisingal, Y. Rachuri, Y. Gu, Y. Choe and D. W. Park, *Chem. Eng. J.*, 2020, **386**, 121700.
- 43 J. Lan, Y. Qu, X. Zhang, H. Ma, P. Xu and J. Sun, *J. CO<sub>2</sub> Util.*, 2020, **35**, 216–224.
- 44 M. Liu, K. Gao, L. Liang, J. Sun, B. Li Sheng and M. Arai, *Catal. Sci. Technol.*, 2016, **6**, 6406.
- 45 Y. H. Li, S. L. Wang, Y. C. Su, B. T. Ko, C. Y. Tsai and C. H. Lin, *Dalton Trans.*, 2018, **47**, 9474–9481.
- 46 N. Seal, M. Singh, S. Das, R. Goswami, B. Pathak and S. Neogi, *Mater. Chem. Front.*, 2021, **5**, 979–994.
- 47 P. Patel, B. Parmar, R. S. Pillai, A. Ansari, N. H. Khan and E. Suresh, *Appl. Catal., A*, 2020, **590**, 117375.
- 48 P. Patel, B. Parmar, R. I. Kureshy, N. H. Khan and E. Suresh, *Dalton Trans.*, 2018, **47**, 8041–8051.
- 49 Y. B. N. Tran, P. T. K. Nguyen, Q. T. Luong and K. D. Nguyen, *Inorg. Chem.*, 2020, **59**, 16747–16759.
- 50 Y. Li, X. Zhang, J. Lan, P. Xu and J. Sun, *Inorg. Chem.*, 2019, **58**, 13917–13926.
- 51 S. Senthilkumar, M. S. Maru, R. S. Somani, H. C. Bajaj and S. Neogi, *Dalton Trans.*, 2018, **47**, 418–428.

